

See discussions, stats, and author profiles for this publication at: <https://www.researchgate.net/publication/273153836>

Elemental Carbon and Polycyclic Aromatic Compounds in a 150-Year Sediment Core from Lake Qinghai, Tibetan Plateau, China: Influence of Regional and Local Sources and Transport Path...

ARTICLE in ENVIRONMENTAL SCIENCE AND TECHNOLOGY · MARCH 2015

Impact Factor: 5.33 · DOI: 10.1021/es504568m · Source: PubMed

CITATIONS

3

READS

200

11 AUTHORS, INCLUDING:



Yongming M Han

Chinese Academy of Sciences

77 PUBLICATIONS 1,545 CITATIONS

SEE PROFILE



Chong Wei

Chinese Academy of Sciences

12 PUBLICATIONS 21 CITATIONS

SEE PROFILE



Junji Cao

Chinese Academy of Sciences

390 PUBLICATIONS 8,047 CITATIONS

SEE PROFILE



Z D Jin

Chinese Academy of Sciences

148 PUBLICATIONS 1,607 CITATIONS

SEE PROFILE

Elemental Carbon and Polycyclic Aromatic Compounds in a 150-Year Sediment Core from Lake Qinghai, Tibetan Plateau, China: Influence of Regional and Local Sources and Transport Pathways

Y. M. Han,^{*,†,‡,§,||} C. Wei,^{†,‡} B. A. M. Bandowe,^{||} W. Wilcke,^{||,⊥} J. J. Cao,^{†,‡} B. Q. Xu,[#] S. P. Gao,[#] X. X. Tie,^{†,‡} G. H. Li,^{†,‡} Z. D. Jin,[‡] and Z. S. An^{‡,||}

[†]Key Laboratory of Aerosol Chemistry & Physics and [‡]SKLLQG, Institute of Earth Environment, Chinese Academy of Sciences, 710061 Xi'an, China

^{||}Joint Center for Global Change Studies, Beijing 100875, China

^{||}Geographic Institute, University of Berne, Hallerstrasse 12, 3012 Berne, Switzerland

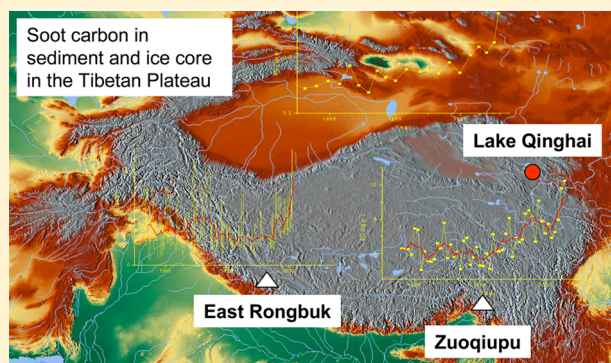
[⊥]Institute of Geography and Geoecology, Karlsruhe Institute of Technology (KIT), Reinhard-Baumeister-Platz 1, 76131 Karlsruhe, Germany

[#]Key Laboratory of Tibetan Environment Changes and Land Surface Processes, Institute of Tibetan Plateau Research, Chinese Academy of Sciences, 100101 Beijing, China

[§]Lamont-Doherty Earth Observatory of Columbia University, Palisades, New York 10964, United States

Supporting Information

ABSTRACT: Elemental carbon (EC) and polycyclic aromatic compounds (PACs) are potential proxies for the reconstruction of change in human activities and the origin of air masses in historic times. In this study, the historic deposition of char and soot (the two subtypes of EC) and PACs in a 150-year sediment core from different topographic subbasins of Lake Qinghai on the Qinghai Tibetan Plateau (QTP) were reconstructed. The objective was to explore how the variations in the concentrations of EC and PACs, in the ratios of char to soot and of oxygenated polycyclic aromatic hydrocarbons (OPAHs) to parent PAHs, and in the composition of the PAC mixtures reflect historical changes in climate and human activity and the origin of air masses arriving at the QTP. The deposition fluxes of soot in the different subbasins were similar, averaging 0.18 (range of 0.15–0.25) and 0.16 (0.13–0.23) g m⁻² year⁻¹, respectively, but they varied for char (averaging 0.11 and 0.22 g m⁻² year⁻¹, respectively), suggesting ubiquitous atmospheric deposition of soot and local river inputs of char. The different vertical distributions of the char/soot ratios in the different subbasins can be interpreted in terms of the different transport mechanisms of char and soot. An abrupt increase in soot concentrations since 1980 coincides with results from the QTP ice cores that were interpreted to be indicative of soot transport from South Asia. Similar concentration patterns of PAHs with soot and 9,10-anthraquinone/anthracene (9,10-AQ/ANT) ratios all >2.0 suggest regional PAC sources. Increasing PAH/soot ratios and decreasing 9,10-AQ/ANT ratios since the beginning of the 1970s indicate increasing local emissions. The historical trends of these diagnostic ratios indicate an increase in the fossil-fuel contribution since the beginning of the 1970s. The increase of perylene concentrations with increasing core depth and the ratio of perylene to its penta-aromatic isomers indicate that perylene originates mainly from in situ biogenic diagenesis. We demonstrate that the concentrations of EC, char, soot, and PACs in sediments can be used to reconstruct local, regional, and remote sources and transport pathways of pollutants to the QTP.



1. INTRODUCTION

Elemental carbon (EC) and polycyclic aromatic compounds (PACs) are produced by the incomplete combustion of fossil fuels and biomass.^{1,2} EC and PACs are markers for biomass burning in preindustrial times^{1,3} and useful indicators of human activities in the modern and industrial times.^{4,5} EC is composed of char and soot corresponding to combusted solid residues and clusters of carbon particles formed by gas-phase processes,

respectively.^{1,6} Because of the differences in their particle sizes and chemophysical and optical properties,⁷ char and soot have different environmental implications. Char, usually consisting of

Received: September 18, 2014

Revised: February 25, 2015

Accepted: March 2, 2015

larger particles, generally deposits on surfaces within a short distance from the emission source and thus reflects local combustion processes, whereas the submicrometer-sized soot particles can be transported great distances and render the atmosphere an important reservoir.⁶ EC records are especially sparse in China.^{3–5} In addition, most of these existing records do not differentiate between char and soot (except for a study in eastern China,⁵ which showed that the soot history reflects the industrialization of China well), thereby missing important information regarding the sources, transport, and climatic effects of char and soot.

Combustion is the major source of polycyclic aromatic hydrocarbons (PAHs), although some diagenetic and biological processes might also contribute.⁸ PAH derivatives such as oxygenated PAHs (OPAHs) and azaarenes (AZAs, nitrogen heterocyclic polycyclic aromatic compounds) are emitted together with PAHs from combustion activities (primary sources). However, OPAHs are also formed in the environment by reactions between parent PAHs and oxidants (e.g., O₃, OH[•], and NO[•]), as well as photolysis and microbial degradation of parent PAHs.⁹ PAHs have been the subject of many studies because of their mutagenic and/or carcinogenic properties.^{10,11} PAHs have been used as proxies for past variations in human activity because they are fire markers.^{12–14} The historical deposition of PAHs in lake sediments and other environmental archives has also been studied extensively worldwide and in China,^{15–17} even in our study area of Lake Qinghai.¹⁸ However, OPAHs and AZAs have seldom been studied in China, even though the simultaneous determination of OPAHs together with their parent PAHs in dated sediment cores offers the opportunity to use the ratio of OPAHs to their parent PAHs as an indicator of the origin of the air mass during historical deposition times. The ratios of OPAHs to their parent PAHs can help to further refine our understanding of whether the human and climatic impacts, as recorded in remote environmental archives, such as the Qinghai–Tibetan Plateau (QTP) region, originate from local, regional, or long-range sources.

The QTP is the highest plateau in the world (average elevation of 4000–5000 m above sea level) and is a relatively pristine area. Because of the high elevation of this plateau, air masses on the QTP can easily enter into the top of the atmosphere and be transported worldwide,¹⁹ so the state of atmospheric pollution above the plateau is globally important. The plateau also harbors the world's largest glaciers after the Arctic and Antarctic, and the deposition of light-absorbing pollutants, such as soot,^{20,21} onto ice surfaces can promote the melting and cause the shrinkage of glaciers. Lake Qinghai is located at the edge of the northeastern QTP, where both the Asian (southwestern and eastern) summer monsoon (ASM, with a humid air atmosphere) and the westerly winds (passing through an arid atmosphere)²² influence the wind regime [Figure S1, Supporting Information (SI)]. The ASM circulation reaches this region in summer, whereas the westerly winds dominate in winter, resulting in a clear seasonality of precipitation.

The objectives of this study are to (1) reconstruct the deposition histories of EC, char, soot, PAHs, OPAHs, and AZAs as indicators of the historical variations of human activities and climate; (2) infer sources and transport paths for these combustion-derived materials; and (3) assess the relationships between EC, char, soot, and PACs to identify the drivers of PAH, OPAH, and AZA patterns in the sediments of Lake Qinghai.

2. EXPERIMENTAL PROCEDURE

A piggyback horst separates Lake Qinghai into two subbasins (Figure S1, SI). Gangcha County, with a population of 42000 located in the northern part of the Qinghai catchment, hosts the largest number of residents around the lake. Seven large rivers flow into the lake, of which four main rivers (Buha, Ha'ergai, Quanji, and Shaliu) in the northern and northwestern parts (Figure S1B, SI) contribute over 80% of the total annual fluvial sediment inputs.²³ We could not use the samples of two previous cores (QH03-02 and QH03-14, collected in the two sub-basins in July 2003, chronologies reported²⁴) for PAC analysis because they were dried at 35 °C. Therefore, a new sediment core (QH11-1), from the same site as QH03-02 in the southern part, was collected in September 2011 to compare the transport differences of carbon fractions, especially for char and soot in the two subbasins. Core QH11-1 was dated using ¹³⁷Cs, ²¹⁰Pb, and ²²⁶Ra analyses (see the SI, including Figure S2), and its average sedimentation rate was similar to that of QH03-02.²⁴ EC, char, and soot concentrations of sediments from QH11-1 and QH03-14 were quantified using the IMPROVE (Interagency Monitoring of Protected Visual Environments) method following Han et al.⁵ The concentrations of 29 parent and alkyl PAHs (including perylene here), 15 OPAHs, and 4 AZAs from QH11-1 were determined following the approach of Bandowe and co-workers.^{25,26} Details of the sampling, dating, analytical procedures, and quality assurance/control for the carbon fractions and PAC analyses are further explained in the Supporting Information.

3. RESULTS AND DISCUSSION

3.1. Core Chronology. The chronology of sediment core QH03-14 in the northern basin was published by Jin et al.²⁴ and was directly used in our study. For core QH11-1 in the southern basin, the chronology obtained from the constant-rate-of-supply (CRS) ²¹⁰Pb model^{27,28} indicated that the ¹³⁷Cs peak occurs at AD 1977 ± 3.4 (Figure S2C, SI). However, the 3.75-cm sediment depth corresponds to AD 1966 ± 4.4. Calculating the ¹³⁷Cs flux using the CRS-derived mass accumulation rate (MAR) data demonstrates that the shape of the ¹³⁷Cs peak becomes very broad and it is difficult to determine where the maximum flux is. In addition, the constrained model²⁸ forcing the chronology through the ¹³⁷Cs fix-point (3.75 cm = AD 1963; Figure S2D, SI) yielded a very similar chronology to the unconstrained model.²⁷ Therefore, the chronology obtained from the unconstrained CRS model²⁷ was used in this study.

3.2. Concentrations of EC, Char, and Soot. Figure 1 reveals different historical variations for EC and char but similar variations for soot in the two subbasins of Lake Qinghai. The EC and char concentrations before 1950 show relatively small variations, averaging 0.50 (range: 0.40–0.68 mg g⁻¹) and 0.25 mg g⁻¹ (range: 0.18–0.45 mg g⁻¹), respectively, in the northern sub-basin, and 0.45 mg g⁻¹ (range: 0.39–0.57 mg g⁻¹) and 0.20 mg g⁻¹ (range: 0.14–0.30 mg g⁻¹), respectively, in the southern sub-basin. However, after 1990, the northern core shows a sharp increase (approximately 3 times higher than those before 1990) in EC and char concentrations, with a maximum of 1.45 mg g⁻¹ in the top 0–0.5-cm increment of the sediment core. This is consistent with more human activities and lacustrine inputs in the northern part, whereas in the southern core, the EC and char concentrations decreased slightly during this period.

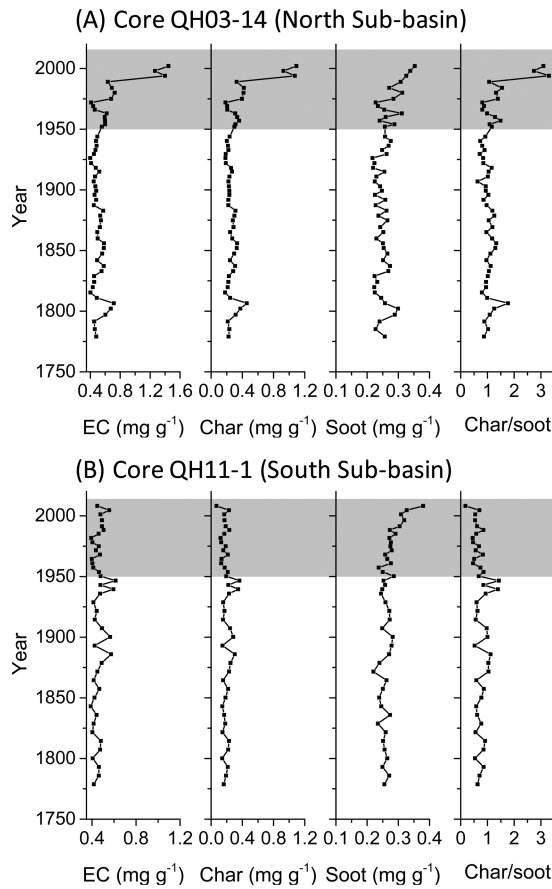


Figure 1. Comparison of the vertical distributions of EC, char, soot, and the char/soot ratio in (A) sediment core QH03-14 (northern subbasin with more anthropogenic inputs) and (B) sediment core QH11-1 (southern subbasin). The shaded portion highlights the period since 1950. Temporal variations of the char and soot fluxes in the two sediment cores are shown in Figure S4 (SI).

For soot, relatively constant concentrations between 0.2 and 0.3 mg g^{-1} were observed in the two subbasins before 1950, with a small increase between 1950 and 1980, which is similar to the anthropogenic Pb profile.²⁴ Since 1980, a sharp increase in both the soot concentrations and the deposition fluxes occurred (maximum in the top 0–0.5 cm) in the two subbasins, although there were fluctuations in the northern part. The average soot concentrations in the two subbasins were similar, at 0.26 and 0.27 mg g^{-1} in the northern and southern parts, respectively.

The EC concentrations are at the lower end of the range of values reported for lake sediments of China,^{3–5} as well as of those reported worldwide using different methods^{17,29–31} (Table 1). Interestingly, the soot concentrations in sediments from different locations in China are all similar; the average concentrations vary from 0.20 to 0.27 mg g^{-1} , with the exception of Lake Taihu (0.42 mg g^{-1}), which is located in the strongly industrialized region of eastern China. The char concentrations in Lake Qinghai sediments are generally lower than those in other published studies from China, in good agreement with the fact that emissions from local human activities are small in this pristine area. Deposition fluxes of EC, char, and soot show regional differences among the different locations, with low fluxes in remote areas, such as Lake Qinghai and Lake Nam Co,⁴ and high fluxes in more populated locations, such as Taihu.⁵ This distribution pattern is

Table 1. Comparison of Concentrations and Deposition Fluxes of EC, Char, and Soot Ratios in Lake Qinghai with Other Records Worldwide

| area | description | concentration (mg g^{-1}) | | | deposition flux ($\text{g m}^{-2} \text{ year}^{-1}$) | | | method |
|---------------------------------|--|--------------------------------------|---------------------|---------------------|---|---------------------|---------------------|---------|
| | | EC | char | soot | EC | char | soot | |
| Lake Qinghai (north) | north Tibetan Plateau, past 150 years | 0.40–1.45 (0.57) | 0.18–1.09 (0.31) | 0.22–0.35 (0.26) | 0.27–0.98 (0.39) | 0.12–0.74 (0.21) | 0.15–0.24 (0.18) | IMPROVE |
| Lake Qinghai (south) | central Tibetan Plateau, past 150 years | 0.39–0.61 (0.46) | 0.07–0.36 (0.19) | 0.22–0.38 (0.27) | 0.22–0.36 (0.27) | 0.04–0.21 (0.11) | 0.13–0.20 (0.16) | |
| Lake Daihai ³ | rural mountains, North China, past 150 years | 0.49–1.09 (0.74) | 0.37–4.69 (2.05) | 0.12–0.35 (0.21) | 0.12–0.44 (0.26) | 0.45–6.7 (2.7) | 0.14–0.43 (0.3) | |
| Lake Chao ⁵ | suburban, eastern China, past 150 years | 0.61–2.03 (1.13) | 0.48–1.58 (0.93) | 0.08–0.47 (0.20) | 1.70–5.67 (3.16) | 1.35–4.43 (2.59) | 0.23–1.31 (0.57) | |
| Lake Taihu ⁵ | well-industrialized urban, eastern China, past 150 years | 0.41–1.95 (1.01) | 0.01–1.43 (0.60) | 0.31–1.09 (0.42) | 1.15–6.89 (3.3) | 0.03–5.55 (2.0) | 0.86–3.12 (1.30) | |
| Aspvreten, Sweden ¹⁷ | background area, past 700 years | | | | 0.071–0.4 | | 0.03–4.21 (1.51) | CTO-375 |
| pan-Arctic ²⁹ | Arctic, surface sediments | 0.17–1.5 | | | 0.0013–0.056 | | | |
| lakes in Slovenia ³¹ | Alps, past 100–200 years | 0.09–1.93 | | | 0.3–11 | | | |
| West Pine Pond ³⁰ | rural, New York state, past 150 years | 0.6–8 | | | 0.026–0.77 | | | STN |

particularly pronounced for soot, with its concentrations in sediments decreasing consistently in the order urban > suburban > rural mountain > remote areas (Table 1).

3.3. Sources and Transport Paths of Char and Soot in Lake Qinghai. Although char and soot are both produced from combustion activities, different sources contribute different proportions of char and soot to total EC. In general, biomass burning generates a much higher percentage of char than soot, with a char/soot ratio of >5–10.⁷ The contribution in Lake Qinghai from biomass burning mainly originates from the combustion of yak dung and grass. However, the char/soot ratios in both subbasins before 1980 were between 0.4 and 1.8, which is even lower than those from sediments of Lake Taihu⁵ but close to those from motor vehicle emissions.⁷ Obviously, motor vehicle emissions could not have been the main source in this region at that time because motor vehicles were not present in the study region. This indicates the influence of long-range transport and deposition of the soot fraction of EC on the char/soot ratio in Lake Qinghai.

The ranges of char/soot ratios from 0.18 to 1.43 for the southern subbasin and from 0.63 to 3.30 for the northern subbasin (Figure 1) can be explained by a decoupling of the soot and char sources. The north subbasin, with higher char/soot ratios, is located close to local anthropogenic sources, such as the city of Gangcha (with a population of ~42000). In addition, because all large rivers, including the Buha, which contributes more than 70% of the detrital inputs to Lake Qinghai,²⁴ are located in the northwestern part (Figure S1, SI), fluvial inputs could also be the reason for the high char/soot ratios. The abrupt increase in char/soot ratios in the 1980s for the northern subbasin coincides with the rapid increase in population, the development of the local tourist industry, and the accompanying rapid rise in human activities in this region (Figure S3, SI). However, the char/soot ratios decreased at the same time for the southern subbasin (Figure 1), which might be associated with the weakening of the summer monsoon shown by the decrease in the lake water level (Figure S4, SI). The similar patterns of concentrations and deposition fluxes for soot in the two sediment cores and the different profiles for char in the two subbasins also support our assumption of local river inputs of char and regional atmospheric deposition of soot into the lake [Figure 1, Figure S5 (SI), and Table 1].

Comparison of soot concentrations with the published EC history from ice core records in the QTP (which cover only the past 50 years and for which Indian EC sources are assumed^{21,32,33}) reveals similar EC patterns in the ice and Lake Qinghai sediment cores. This is particularly true since 1980, the year in which a sharp increase in EC concentrations in ice cores of the Tibetan Plateau²¹ and the sediment core of Lake Qinghai was observed. Rapid industrialization in China began in the late 1970s,⁵ only a little earlier than the increase in soot concentrations in Lake Qinghai. We suggest that both the Indian emissions and the inland EC emissions from eastern China contribute to soot deposition in this region, as the study area is located at the boundary of both the eastern Asian monsoon and the Indian monsoon.²² Previous modeling³⁴ suggested that southern and eastern Asia contribute 67% and 17%, respectively, to the total EC transported to the Tibetan Plateau.

3.4. Historic Variation of PAHs, OPAHs, and AZAs. The temporal variations in the concentrations of $\Sigma 28$ PAHs (total concentration of all analyzed PAHs without perylene; Figure 2), low-molecular-weight (LMW) PAHs (two- to three-ring

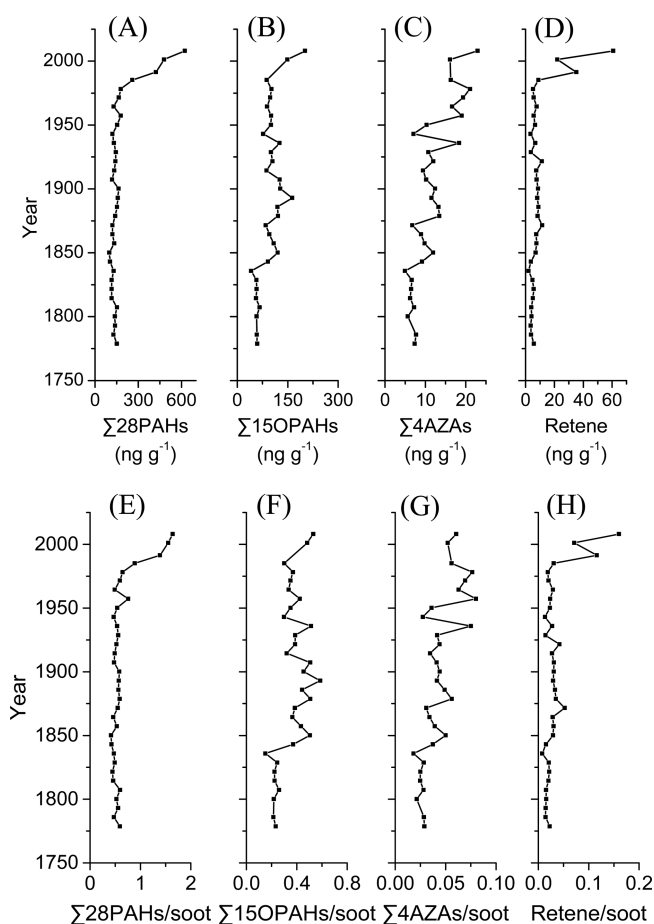


Figure 2. (A–D) Vertical distributions and (E–H) concentration ratios to soot (which are indicative of variations in atmospheric deposition and local inputs) of (A,E) $\Sigma 28$ PAHs (all analyzed PAHs without perylene), (B,F) $\Sigma 15$ oxygenated PAHs, (C,G) $\Sigma 4$ azaarenes (AZAs), and (D,H) retene.

parent PAHs), and high-molecular-weight (HMW) PAHs (four- to seven-ring parent PAHs; Figure S6, SI) are similar to that of soot, with relatively stable concentrations before 1980 and a sharp increase thereafter. However, the temporal variation of $\Sigma 28$ PAHs in the Lake Qinghai sediment core is different from that of char (Figures 1 and 2). This suggests that the parent PAHs might also originate from long-range atmospheric transport associated with soot. Soot has sources similar to those of PAHs and a high sorption capacity for PAHs. The long-range transport of PAHs to Lake Qinghai is further supported by the 9,10-anthraquinone/anthracene (9,10-AQ/ANT) ratio (see section 3.5). The increase in the $\Sigma 28$ PAHs/soot ratio since the 1990s marks a partial decoupling of the joint deposition of PAHs and soot from distant sources. Since the 1980s, local contributions of PAHs likely have increased, because of the increase in population, tourists, and electricity generation in Qinghai Province (Figure S3, SI). Char concentrations show a negative correlation with those of $\Sigma 28$ PAHs (Table S2, SI), indicating different controlling factors on char and PAH deposition, which might involve different transport distances, different local sources, and different formation pathways (see section 3.4).

The $\Sigma 15$ OPAHs concentration also increased in recent times, but in a different manner from that of $\Sigma 28$ PAHs (Figure 2). The first increase in the $\Sigma 15$ OPAHs and $\Sigma 4$ AZAs

concentrations occurred around ~1850 (Figure 2), at the beginning of the Industrial Revolution in western Europe. The long-range transport of pollutants by the westerly winds (the northern branch surrounding the QTP; see Xu et al.²¹) to the QTP was shown in previous studies.^{21,35} The strong correlation between the $\Sigma 15\text{OPAHs}$ concentration and retene, an indicator of biomass burning³⁶ (Table S2, SI), suggests that primary combustion, especially from biomass burning, might be one of the main sources for OPAHs in the old part of the sediment core. The peak of $\Sigma 15\text{OPAHs}$ in the 1910s occurred together with high concentrations of $\Sigma 4\text{AZAs}$ and $\Sigma \text{Comb-PAHs}$ ³⁷ [combustion-derived PAHs; see footnote of Table S1 (SI) for definition] and Pb.²⁴ The increase in Pb concentrations at that time has been attributed to enhanced agricultural activities²⁴ that used fires for land reclamation.

Similarly to the concentrations of $\Sigma 28\text{PAHs}$, those of $\Sigma 4\text{AZAs}$ also increased in the upper part of the sediment core, reaching the highest values in the 21st century (Figure 2). The $\Sigma 4\text{AZAs}$ concentrations ranged from 5.0 to 23.0 ng g⁻¹ and averaged 11.6 ng g⁻¹, which is lower than the concentration range reported for Danshuei River, Taiwan, of 3.7–154 ng g⁻¹.³⁸ It is widely believed that PAHs and AZAs have similar anthropogenic sources, but their fates in the environment are different.³⁹ In this study, the PAH concentrations were closely correlated with those of three-ring AZAs ($r = 0.51$, $p = 0.002$) but poorly correlated with those of two-ring AZAs ($r = 0.16$, $p = 0.385$). This suggests that three-ring AZAs have sources and fates similar to those of PAHs, whereas two-ring AZAs have different sources and/or fates in the sediment because of the higher solubility of two-ring AZAs in water.³⁹ Before the 1960s, when long-range-transported PAHs dominated, there were relatively more two-ring than three-ring AZAs, whereas after the end of the 1960s, with the increase in local inputs, three-ring AZAs became more prominent (see the change in slopes in Figure S7, SI).

3.5. Covariation of PACs with TOC, EC, Char, and Soot.

The closest correlation coefficient (Table S2 and Figure S8, SI) exists between the concentrations of soot and $\Sigma 28\text{PAHs}$ ($r = 0.84$, $p < 0.001$), followed by TOC with $\Sigma 28\text{PAHs}$ and $\Sigma 15\text{OPAHs}$ ($r = 0.61$, $p < 0.01$). Although close correlations between the concentrations of PAHs and EC have been reported by others and attributed to coemission, cotransport, and sorption of these materials,⁴⁰ the EC and char concentrations in Lake Qinghai sediments correlate only weakly with those of $\Sigma 28\text{PAHs}$ and $\Sigma 15\text{OPAHs}$. Nam et al.⁴⁰ suggested that the associations between EC and PAHs are more important in closer proximity to combustion sources, whereas PAH partitioning to soil organic matter (measured as TOC) is more important in remote sites. However, because both soot and PAHs can originate from long-range atmospheric transport, the PAH–soot partitioning is likely to be more important in remote areas. The mixing of char and soot in EC might obscure the correlation between the concentrations of EC and $\Sigma 28\text{PAHs}$, emphasizing the importance to differentiate between char and soot.

3.6. Temporal Trends of PAC Composition Patterns and Concentration Ratios. Numerous markers have been used to infer different sources of PAHs. For example, retene was suggested as an indicator of biomass burning,³⁶ and indeno[1,2,3-*cd*]pyrene, benzo[*g,h,i*]perylene, and coronene were proposed as indicators for oil combustion emissions.⁴¹ The concentrations of indeno[1,2,3-*cd*]pyrene, benzo[*g,h,i*]perylene, and coronene began to increase in ~1980 (Figure S6,

SI), coinciding with increasing oil production (or use) in Qinghai Province (Figure S3, SI). The retene concentrations increased only beginning in the late-1990s (Figure 2), when the “Scenic district of Lake Qinghai” was established as a tourist attraction. Since then, the number of tourists has increased sharply (Figure S3, SI), resulting in increased use of yak dung for residential heating in this area.

A previous study suggested that the 9,10-AQ/ANT concentration ratio remains constant in sediments, in contrast to that in the atmosphere, because sediments are not exposed to UV radiation⁴² and that a 9,10-AQ/ANT ratio greater than 1 indicates primary input from atmospheric deposition whereas a 9,10-AQ/ANT ratio less than 1 means lacustrine input.⁴² In this study, the 9,10-AQ/ANT ratios (Figure 3) ranged from 2.4

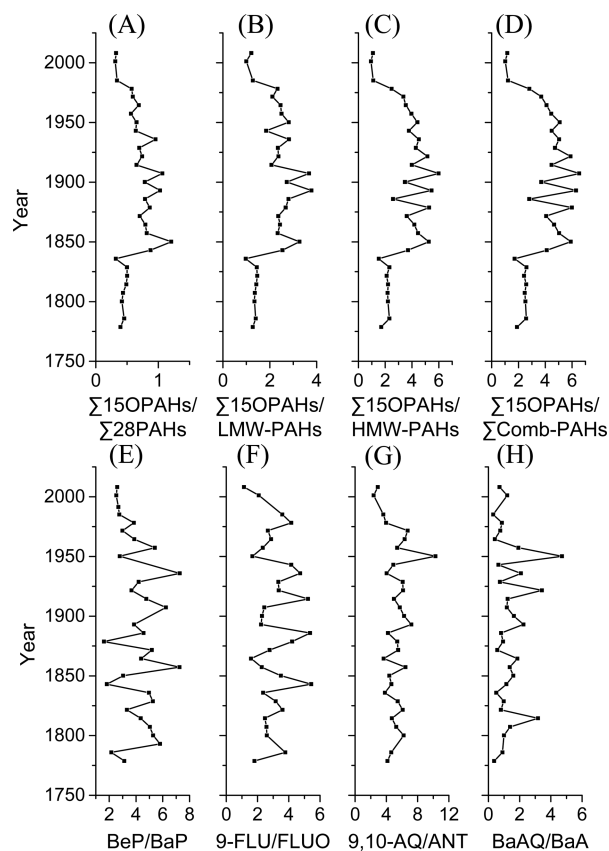


Figure 3. Vertical distributions of the concentration ratios of (A) total OPAHs to total PAHs, (B) total OPAHs to LMW PAHs, (C) total OPAHs to HMW PAHs, (D) total OPAHs to combustion-derived PAHs ($\Sigma \text{Comb-PAH}$), and (E–H) individual OPAHs to their parent PAHs. BeP/BaP, 9-FLU/FLUO, 9,10-AQ/ANT, and BaAQ/BaA refer to benzo[*e*]pyrene/benzo[*a*]pyrene, 9-fluorenone/fluorene, 9,10-anthraquinone/anthracene, and benzo[*a*]anthracene-7,12-dione/benzo[*a*]anthracene, respectively.

to 10.3 with an average of 5.2, indicating the dominance of atmospheric deposition. Since the beginning of the 1970s, the ratios have decreased, consistent with the time of increase in $\Sigma 28\text{PAHs}$ concentrations originating from local inputs (see section 3.3), suggesting increasing inputs of pollutants from local emissions. Other ratios of individual OPAHs to their parent PAHs show temporal trends similar to that of the 9,10-AQ/ANT ratio, whereas this is not the case for the $\Sigma 15\text{OPAHs}/\Sigma 28\text{PAHs}$ ratio (Figure 3). Before the 1840s, the $\Sigma 15\text{OPAHs}/\Sigma 28\text{PAHs}$ ratios were low (i.e., 0.44), and

the ratios then increased and reached the highest value of 1.21 in the 1870s. Thereafter, the $\sum 15\text{OPAHs}/\sum 28\text{PAHs}$ ratios in the sediments decreased until recently. This change might be associated with secondary formation of OPAHs during long-range transport. Low $\sum 15\text{OPAHs}/\sum 28\text{PAHs}$ ratios before the 1840s might indicate the dominance of background local inputs. After the 1870s, the stepwise increases in industrialization in China, such as the Westernization Movement (1861–1895) and the Golden Decade (1927–1937),⁴³ might have resulted in the decrease of the $\sum 15\text{OPAHs}/\sum 28\text{PAHs}$ ratios because of the increase in local compared to regional emissions, especially after the political reform and economic opening of China in the later 1970s.

3.7. Evidence of Nonpyrogenic Sources of Perylene.

Perylene is absent from the surficial sediments of Lake Qinghai, and its concentration generally increases with depth and reaches 39.5 ng g^{-1} at the lake bottom. The surficial perylene concentrations are lower than the sum of the concentrations of its penta-aromatic isomer PAHs (benzo[*a*]pyrene, benzo[*e*]pyrene, and benzo[*b,j,k*]fluoranthene; Figure S9, SI), whereas the perylene concentrations were higher than the sum of these isomers in deeper sediments. These results suggest that most of the perylene in Lake Qinghai likely originates mainly from in situ biogenic diagenesis under anoxic conditions.⁴⁴ The contribution of the perylene concentrations to the total concentrations of all penta-aromatic isomers (PAIs) is $\sim 8\%$ in surficial sediments and increases with depth to values of $>10\%$ (Figure S10, SI), which are considered indicative of a diagenetic source of perylene.¹⁸ The concentration ratios of perylene to TOC, PAI, and $\sum 28\text{PAHs}$ generally increase with increasing sediment depth and therefore age, suggesting the continuous formation of perylene over time (Figure S10, SI). Furthermore, it can be concluded that the formation of perylene in Lake Qinghai is a first-order reaction (Figure 4), implying that the production of perylene depends simply on the availability of precursors and the age of the sediment.

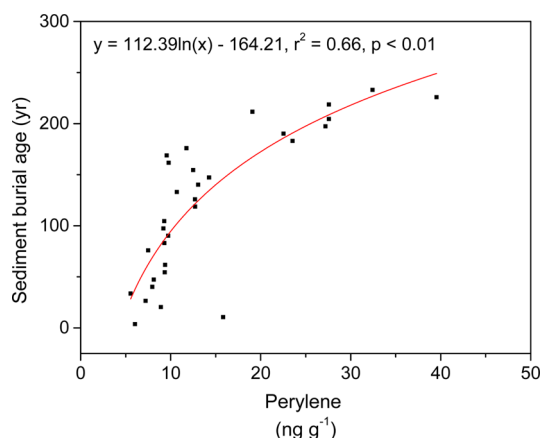


Figure 4. Relationship between perylene concentration and sediment burial age in Lake Qinghai.

Perylene has a significant negative correlation with TOC ($r = -0.51$, $p = 0.003$) and C/N ratio ($r = -0.50$, $p = 0.004$), supporting our assumption that some components of TOC are precursors of perylene formation. The organic matter in the sediment of Lake Qinghai originates mainly from terrestrial plants, such as alpine meadows and steppe grasses, shown by the C/N ratio (ranging from 9.1 to 23.4 and averaging 14.4)

and *n*-alkane data.⁴⁵ Perylenequinone, one of the probable precursors of perylene in “P-type” humic acid, can occur in the podzolic grassland soils surrounding Lake Qinghai⁴⁶ and thus could have contributed to perylene formation in Lake Qinghai.

■ ASSOCIATED CONTENT

Supporting Information

Methods section. Locations of sediment cores (Figure S1) and sediment chronology (Figure S2). Temporal variations in human activities (Figure S3), lake surface size (Figure S4), char and soot fluxes (Figure S5), and concentrations of selected PACs (Figure S6). Relationships between the concentrations of two-ring and three-ring AZAs and PAHs (Figure S7) and between the concentrations of PAHs and AZAs char (soot) (Figure S8). Vertical distributions of the concentrations of perylene and its combustion-derived isomers in sediments (Figure S9). Perylene/PAI, perylene/TOC, and perylene/ $\sum 28\text{PAHs}$ concentration ratios, together with C/N ratios (Figure S10). This material is available free of charge via the Internet at <http://pubs.acs.org>.

■ AUTHOR INFORMATION

Corresponding Author

*E-mail: yongming@ieecas.cn.

Notes

The authors declare no competing financial interest.

■ ACKNOWLEDGMENTS

We thank Prof. Martin Grosjean of the University of Bern for his assistance in the chronology reconstruction in this study. This study was supported by the NSF of China (41273140 and 41473119), the National Basic Research Program of China (2013CB955900), the Chinese Academy of Sciences (XDA05100402 and KZZD-EW-04), and the Swiss National Science Foundation (SNF 200021_131938/1).

■ REFERENCES

- (1) Goldberg, E. D. *Black Carbon in the Environment*; John Wiley & Sons, Inc.: New York, 1985.
- (2) Cornelissen, G.; Breedveld, G. D.; Kalaitzidis, S.; Christanis, K.; Kibsgaard, A.; Oen, A. M. P. Strong sorption of native PAHs to pyrogenic and unburned carbonaceous geosorbents in sediments. *Environ. Sci. Technol.* **2006**, *40* (4), 1197–1203.
- (3) Han, Y. M.; Marlon, J.; Cao, J. J.; Jin, Z. D.; Aun, Z. S. Holocene linkages between char, soot, biomass burning and climate from Lake Daihai, China. *Global Biogeochem. Cycles* **2012**, *26*, GB4017.
- (4) Cong, Z.; Kang, S.; Gao, S.; Zhang, Y.; Li, Q.; Kawamura, K. Historical trends of atmospheric black carbon on Tibetan Plateau as reconstructed from a 150-year lake sediment record. *Environ. Sci. Technol.* **2013**, *47* (6), 2579–2586.
- (5) Han, Y. M.; Cao, J. J.; Yan, B. Z.; Kenna, T. C.; Jin, Z. D.; Cheng, Y.; An, Z. S. Comparison of elemental carbon in lake sediments measured by TOR, TOT and CTO methods and 150-year pollution history in Eastern China. *Environ. Sci. Technol.* **2011**, *45* (12), S287–S293.
- (6) Masiello, C. A. New directions in black carbon organic geochemistry. *Mar. Chem.* **2004**, *92* (1–4), 201–213.
- (7) Han, Y. M.; Cao, J. J.; Lee, S. C.; Ho, K. F.; An, Z. S. Different characteristics of char and soot in the atmosphere and their ratio as an indicator for source identification in Xi'an, China. *Atmos. Chem. Phys.* **2010**, *10* (2), 595–607.
- (8) Wilcke, W. Polycyclic aromatic hydrocarbons (PAHs) in soil—A review. *J. Plant Nutr. Soil Sci.* **2000**, *163* (3), 229–248.
- (9) Albinet, A.; Leoz-Garziandia, E.; Budzinski, H.; Villenave, E.; Jaffrezo, J. L. Nitrated and oxygenated derivatives of polycyclic

aromatic hydrocarbons in the ambient air of two French alpine valleys: Part 1: Concentrations, sources and gas/particle partitioning. *Atmos. Environ.* **2008**, *42* (1), 43–54.

(10) Pedersen, D. U.; Durant, J. L.; Taghizadeh, K.; Hemond, H. F.; Lafleur, A. L.; Cass, G. R. Human cell mutagens in respirable airborne particles from the Northeastern United States. 2. Quantification of mutagens and other organic compounds. *Environ. Sci. Technol.* **2005**, *39* (24), 9547–9560.

(11) Alam, M. S.; Delgado-Saborit, J. M.; Stark, C.; Harrison, R. M. Investigating PAH relative reactivity using congener profiles, quinone measurements and back trajectories. *Atmos. Chem. Phys.* **2014**, *14* (5), 2467–2477.

(12) Musa Bandowe, B. A.; Srinivasan, P.; Seelge, M.; Sirocko, F.; Wilcke, W. A 2600-year record of past polycyclic aromatic hydrocarbons (PAHs) deposition at Holzmaar (Eifel, Germany). *Palaeogeogr., Palaeoclimatol., Palaeoecol.* **2014**, *401* (0), 111–121.

(13) Azoury, S.; Tronczynski, J.; Chiffolleau, J. F.; Cossa, D.; Nakhle, K.; Schmidt, S.; Khalaf, G. Historical records of mercury, lead, and polycyclic aromatic hydrocarbons depositions in a dated sediment core from the Eastern Mediterranean. *Environ. Sci. Technol.* **2013**, *47* (13), 7101–7109.

(14) Petrisic, M. G.; Muri, G.; Ogrinc, N. Source identification and sedimentary record of polycyclic aromatic hydrocarbons in Lake Bled (NW Slovenia) using stable carbon isotopes. *Environ. Sci. Technol.* **2013**, *47* (3), 1280–1286.

(15) Guo, J.; Wu, F.; Luo, X.; Liang, Z.; Liao, H.; Zhang, R.; Li, W.; Zhao, X.; Chen, S.; Mai, B. Anthropogenic input of polycyclic aromatic hydrocarbons into five lakes in Western China. *Environ. Pollut.* **2010**, *158* (6), 2175–2180.

(16) Yan, B. Z.; Abrajano, T. A.; Bopp, R. F.; Chaky, D. A.; Benedict, L. A.; Chillrud, S. N. Molecular tracers of saturated and polycyclic aromatic hydrocarbon inputs into Central Park Lake, New York City. *Environ. Sci. Technol.* **2005**, *39* (18), 7012–7019.

(17) Elmquist, M.; Zencak, Z.; Gustafsson, O. A 700 year sediment record of black carbon and polycyclic aromatic hydrocarbons near the EMEP air monitoring station in Aspvreten, Sweden. *Environ. Sci. Technol.* **2007**, *41*, 6926–6932.

(18) Wang, X.; Yang, H.; Gong, P.; Zhao, X.; Wu, G.; Turner, S.; Yao, T. One century sedimentary records of polycyclic aromatic hydrocarbons, mercury and trace elements in the Qinghai Lake, Tibetan Plateau. *Environ. Pollut.* **2010**, *158* (10), 3065–3070.

(19) Fu, R.; Hu, Y. L.; Wright, J. S.; Jiang, J. H.; Dickinson, R. E.; Chen, M. X.; Filipiak, M.; Read, W. G.; Waters, J. W.; Wu, D. L. Short circuit of water vapor and polluted air to the global stratosphere by convective transport over the Tibetan Plateau. *Proc. Natl. Acad. Sci. U.S.A.* **2006**, *103* (15), 5664–5669.

(20) Hansen, J.; Nazarenko, L. Soot climate forcing via snow and ice albedos. *Proc. Natl. Acad. Sci. U.S.A.* **2004**, *101* (2), 423–428.

(21) Xu, B. Q.; Cao, J. J.; Hansen, J.; Yao, T. D.; Joswila, D. R.; Wang, N. L.; Wu, G. J.; Wang, M.; Zhao, H. B.; Yang, W.; Liu, X. Q.; He, J. Q. Black soot and the survival of Tibetan glaciers. *Proc. Natl. Acad. Sci. U.S.A.* **2009**, *106* (52), 22114–22118.

(22) An, Z.; Colman, S. M.; Zhou, W.; Li, X.; Brown, E. T.; Jull, A. J. T.; Cai, Y.; Huang, Y.; Lu, X.; Chang, H.; Song, Y.; Sun, Y.; Xu, H.; Liu, W.; Jin, Z.; Liu, X.; Cheng, P.; Liu, Y.; Ai, L.; Li, X.; Liu, X.; Yan, L.; Shi, Z.; Wang, X.; Wu, F.; Qiang, X.; Dong, J.; Lu, F.; Xu, X. Interplay between the Westerlies and Asian monsoon recorded in Lake Qinghai sediments since 32 ka. *Sci. Rep.* **2012**, *2*, 619.

(23) Xu, H.; Ai, L.; Tan, L.; An, Z. Geochronology of a surface core in the northern basin of Lake Qinghai: Evidence from ^{210}Pb and ^{137}Cs radionuclides. *Chin. J. Geochem.* **2006**, *25*, 301–306.

(24) Jin, Z.; Han, Y.; Chen, L. Past atmospheric Pb deposition in Lake Qinghai, northeastern Tibetan Plateau. *J. Paleolimnol.* **2010**, *43* (3), 551–563.

(25) Bandowe, B. A. M.; Sobocka, J.; Wilcke, W. Oxygen-containing polycyclic aromatic hydrocarbons (OPAHs) in urban soils of Bratislava, Slovakia: Patterns, relation to PAHs and vertical distribution. *Environ. Pollut.* **2011**, *159* (2), 539–549.

(26) Bandowe, B. A. M.; Shukurov, N.; Kersten, M.; Wilcke, W. Polycyclic aromatic hydrocarbons (PAHs) and their oxygen-containing derivatives (OPAHs) in soils from the Angren industrial area, Uzbekistan. *Environ. Pollut.* **2010**, *158* (9), 2888–2899.

(27) Appleby, P. G. Chronostratigraphic techniques in recent sediments. In *Tracking Environmental Change Using Lake Sediments*; Last, W. M., Smol, J. P., Eds.; Kluwer Academic Publishers: Dordrecht, The Netherlands, 2001; Vol. 1, pp 171–203.

(28) von Gunten, L.; Grosjean, M.; Beer, J.; Grob, P.; Morales, A.; Urrutia, R. Age modeling of young non-varved lake sediments: Methods and limits. Examples from two lakes in Central Chile. *J. Paleolimnol.* **2009**, *42* (3), 401–412.

(29) Elmquist, M.; Semiletov, I.; Guo, L. D.; Gustafsson, O. Pan-Arctic patterns in black carbon sources and fluvial discharges deduced from radiocarbon and PAH source apportionment markers in estuarine surface sediments. *Global Biogeochem. Cycles* **2008**, *22*, GB2018.

(30) Husain, L.; Khan, A. J.; Ahmed, T.; Swami, K.; Bari, A.; Webber, J. S.; Li, J. Trends in atmospheric elemental carbon concentrations from 1835 to 2005. *J. Geophys. Res.* **2008**, *113* (D13), D13102.

(31) Muri, G.; Cermelj, B.; Faganeli, J.; Brancelj, A. Black carbon in Slovenian alpine lacustrine sediments. *Chemosphere* **2002**, *46* (8), 1225–1234.

(32) Ming, J.; Cachier, H.; Xiao, C.; Qin, D.; Kang, S.; Hou, S.; Xu, J. Black carbon record based on a shallow Himalayan ice core and its climatic implications. *Atmos. Chem. Phys.* **2008**, *8* (5), 1343–1352.

(33) Wang, M.; Xu, B.; Cao, J.; Tie, X.; Wang, H.; Zhang, R.; Qian, Y.; Rasch, P. J.; Zhao, S.; Wu, G.; Zhao, H.; Joswiak, D. R.; Li, J.; Xie, Y. Carbonaceous aerosols recorded in a Southeastern Tibetan glacier: Variations, sources and radiative forcing. *Atmos. Chem. Phys. Discuss.* **2014**, *14* (13), 19719–19746.

(34) Lu, Z.; Streets, D. G.; Zhang, Q.; Wang, S. A novel back-trajectory analysis of the origin of black carbon transported to the Himalayas and Tibetan Plateau during 1996–2010. *Geophys. Res. Lett.* **2013**, *39* (1), L01809.

(35) Cao, J.; Tie, X.; Xu, B.; Zhao, Z.; Zhu, C.; Li, G.; Liu, S. Measuring and modeling black carbon (BC) contamination in the SE Tibetan Plateau. *J. Atmos. Chem.* **2010**, *67* (1), 45–60.

(36) Ramdahl, T. Retene—A molecular marker of wood combustion in ambient air. *Nature* **1983**, *306* (5943), 580–583.

(37) Hwang, H. M.; Wade, T. L.; Sericano, J. L. Concentrations and source characterization of polycyclic aromatic hydrocarbons in pine needles from Korea, Mexico, and United States. *Atmos. Environ.* **2003**, *37* (16), 2259–2267.

(38) Chen, H.-Y.; Su, C.-C.; Hung, C.-C.; Yeh, T.-C.; Shen, Y.-H.; Tsai, C.-H.; Chen, L.-D.; Gong, G.-C. Occurrence of azaarenes in sediments of the Danshuei River, Taiwan—The use of azaarenes as indicator of anthropogenic source to the estuarine system. *Environ. Toxicol.* **2008**, *23* (1), 25–35.

(39) Osborne, P. J.; Preston, M. R.; Chen, H.-y. Azaarenes in sediments, suspended particles and aerosol associated with the River Mersey estuary. *Mar. Chem.* **1997**, *58* (1–2), 73–83.

(40) Nam, J. J.; Thomas, G. O.; Jaward, F. M.; Steinnes, E.; Gustafsson, O.; Jones, K. C. PAHs in background soils from Western Europe: Influence of atmospheric deposition and soil organic matter. *Chemosphere* **2008**, *70* (9), 1596–1602.

(41) Omar, N.; Bin Abas, M. R.; Ketuly, K. A.; Tahir, N. M. Concentrations of PAHs in atmospheric particles (PM-10) and roadside soil particles collected in Kuala Lumpur, Malaysia. *Atmos. Environ.* **2002**, *36* (2), 247–254.

(42) McKinney, R. A.; Pruell, R. J.; Burgess, R. M. Ratio of the concentration of anthraquinone to anthracene in coastal marine sediments. *Chemosphere* **1999**, *38* (10), 2415–2430.

(43) Lee, C. S. L.; Qi, S.-H.; Zhang, G.; Luo, C.-L.; Zhao, L. Y. L.; Li, X.-D. Seven thousand years of records on the mining and utilization of metals from lake sediments in central China. *Environ. Sci. Technol.* **2008**, *42* (13), 4732–4738.

(44) Silliman, J. E.; Meyers, P. A.; Ostrom, P. H.; Ostrom, N. E.; Eadie, B. J. Insights into the origin of perylene from isotopic analyses

of sediments from Saanich Inlet, British Columbia. *Org. Geochem.* **2000**, *31* (11), 1133–1142.

(45) Duan, Y.; Wu, B.; Xu, L.; He, J.; Sun, T. Characterisation of *n*-alkanes and their hydrogen isotopic composition in sediments from Lake Qinghai, China. *Org. Geochem.* **2011**, *42* (7), 720–726.

(46) Itoh, N.; Hanari, N. Possible precursor of perylene in sediments of Lake Biwa elucidated by stable carbon isotope composition. *Geochem. J.* **2010**, *44* (3), 161.